where x_r and y_r are coordinates in $\sum_R$, x_w and y_w are coordinates in the writing order coordinate system $\sum_W$ as shown in Fig. 4b, H_{char} is the height of the character image pattern, $(x_R + T_R/2, y_R - T_R/2)$ is the center of the writing area, and (X_{char}, Y_{char}) is the center of character in $\sum_W$. Hereafter, if no specific declaration, the coordinates of the control points are those in $\sum_R$.

3.4.1. S_1: *Horizontal stroke.* S_1 is not just a simple straight line. As shown in Fig. 10a, the character for 'king' contains three S_1's. In CCC, these three S_1's are written differently: (1) concave, (2) flat and (3) convex as in (a). In general, to generate the trajectory of the writing brush for this stroke, four control points P_1 to P_4 are necessary. In the case that the number of the control points is less than 4, auxiliary points can be generated according the coordinates of the control points. Auxiliary points B_1 and B_2 are generated from the coordinates of P_1, and E_1 to E_3 from those of P_4. The value of their coordinates are given in detail below.

(i) *Writing the start of* S_1
Trajectory: $B_1(x_1 - 2d_x, y_1 + d_y, z_d - d_{min}) \rightarrow B_2(x_1 + 2d_x, y_1 - d_y, z_d - 1.1d) \rightarrow P_1(x_1, y_1, z_d - d)$.

Note that x_1 and y_1 are coordinates of the control point P_1 and the change of the z-coordinate is to make the tip of the writing brush take the shape as shown in Fig. 9c.

(ii) *Movement of the writing brush*
Trajectory: $P_1 \rightarrow Q_0 \rightarrow Q_1 \rightarrow \cdots \rightarrow Q_M \rightarrow P_4$.

Note that Q_j $(j = 0, 1, \ldots, M)$ is the point on the B-spline curve determined by P_1 to P_4 and the width is $z_d - d$.

(iii) *Writing the end of* S_1
Trajectory: $E_1(x_4 - d_x, y_4 + d_y, z_d - 0.8d) \rightarrow E_2(x_4 + 2d_x, y_4 - 2d_y, z_d - 1.1d) \rightarrow E_3(x_4 - 3d_x, y_4 - d_y, z_d - 0.8d)$.

Note that x_4 and y_4 are coordinates of the control point P_4 and the change of the z-coordinate is to make the end of the stroke take the shape as shown in Fig. 10b. Figure 10c shows the three variations of S_1 written by a robot hand.

3.4.2. S_2: *Vertical stroke.* Figure 11a shows four variations of S_2. The first one from the left is similar to the left falling stroke S_3. The control technique for it is the same with that of S_3 and will be discussed later. The second from the left is

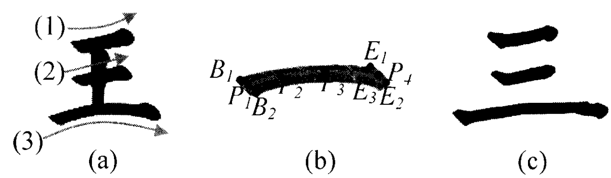

Figure 10. (a) Sample character for 'king' including three S_1s. (b) Trajectory to write S_1. (c) Three S_1s writen by the robot hand.

called an iron post, the third a hanging pin, and the fourth an elephant tooth. The trajectories for these three kinds of vertical strokes are determined by two control points P_1 and P_2. The following shows the trajectories of them.

(i) *Writing the iron post*
Start: the same with that of S_1.
Movement of the writing brush: $P_1(x_1, y_1, z_d - d) \rightarrow P_2(x_2, y_2, z_d - d)$.
End: $E_1(x_1 - d_x, y_1 + d_y, z_d - 0.8d) \rightarrow E_2(x_2 + d_x, y_2 - 2d_y, z_d - 1.1d)$.

(ii) *Writing the hanging pin*
Start: the same with that of S_1.
Movement of the writing brush: $P_1(x_1, y_1, z_d - d) \rightarrow E_1((nx_1 + mx_2)/(m + n), (ny_1 + my_2)/(m + n), z_d - d) \rightarrow P_2(x_2, y_2, z_d - d_{\min})$.
Note that $m : n = P_1E_1 : E_1P_2$ and is in the range from $6 : 1$ to $10 : 1$.

(iii) *Writing the elephant tooth*
Start: the same with that of S_1.
Movement of the writing brush: $P_1(x_1, y_1, z_d - d) \rightarrow P_2(x_2, y_2, z_d - d) \rightarrow E_1(x_2 - d_x, y_2 - d_y, z_d - d_{\min})$.
Figure 11b shows the three variations of S_2 written by a robot hand.

3.4.3. S_0: *Dot stroke.* The dot stroke is very complicated to write even for human calligraphers. Figure 12a shows four variations of S_0. They are called the right inclined dot, rising dot, vertical dot and right falling dot, from left. To express these dots, three control points P_1, P_2 and P_3 are necessary. To determine the trajectories for them, two auxiliary points R_1 and R_2 are inserted between P_1 and P_2 for these dots, except the vertical dot, according to:

$$x_{R_k} = \mp(y_2 - y_1) \times d_x / \|P_1P_2\| + (nx_1 + mx_2)/(m + n), \tag{8a}$$

$$y_{R_k} = \mp(x_2 - x_1) \times d_x / \|P_1P_2\| + (ny_1 + my_2)/(m + n), \tag{8b}$$

where $k = 1, 2$. When $k = 1$, $m : n$ is set to $1 : 2$ and when $k = 2$, $m : n = 2 : 1$. When x_{R_k} takes '$-$' and y_{R_k} takes '$+$' in the first item in (8), (x_{R_k}, y_{R_k}) lies in the left side of line P_1P_2 when moving from P_1 to P_2. Oppositely, (x_{R_k}, y_{R_k}) lies in the right side of line P_1P_2. For the right inclined dot and right falling dot, R_1 and R_2 are set on the left side of the line P_1P_2; for the rising dot, on the right side.

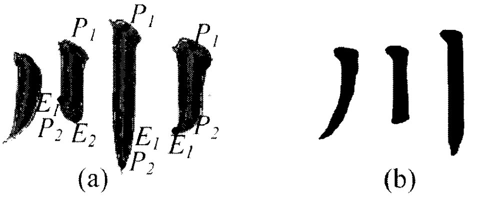

Figure 11. (a) Four variations of S_2. (b) Three S_2s written by the robot hand.

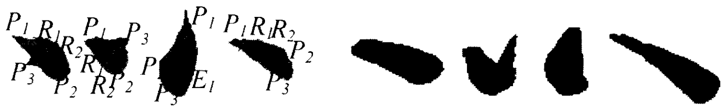

(a) (b)

Figure 12. (a) Four variations of S_0. (b) Four S_0s written by the robot hand.

(i) *Writing the right inclined dot, rising dot and right falling dot*
Start: $B_1(x_1 - d_x, y_1 + d_y, z_d - d_{min}) \rightarrow P_1(x_1, y_1, z_d - d_{min})$ and B_1 is the same as related in S_1.
Movement of the writing brush: $P_1 \rightarrow Q_0 \rightarrow Q_1 \rightarrow \cdots \rightarrow Q_M \rightarrow P_2$.

Note that Q_j $(j = 0, 1, \ldots, M)$ is the point on the B-spline curve determined by P_1, R_1, R_2 and P_2, and the width is controlled by:

$$z_j = z_d - \left(d_{min} + (d - d_{min})\frac{k\delta}{M}\right). \tag{9}$$

End: $P_2(x_2, y_2, z_M) \rightarrow P_3(x_3, y_3, z_d - d_{min})$.

(ii) *Writing the vertical dot*
Start: $B_1(x_1 - d_x, y_1 + d_y, z_d - d_{min}) \rightarrow P_1(x_1, y_1, z_d - d_{min})$, where B_1 is the same as related in S_1.
Movement of the writing brush: $P_1(x_1, y_1, z_d - d_{min}) \rightarrow P_2(x_2, y_2, z_d - d) \rightarrow P_3(x_3, y_3, z_d - d)$.
End: $P_3(x_3, y_3, z_d - d) \rightarrow E_1(x_3 + d_x, y_2, z_d - d_{min})$, where E_1 is generated from P_2 and P_3.

Figure 12b shows the four variations of S_0 written by a robot hand.

3.4.4. S_3: Left falling stroke. The size of the left falling stroke changes from a very short one like a dot to a very long one, depending on the positions located in the different characters. For the short one, it can be expressed by two control points. Here, in general, at least four control points are necessary. If the number of control points is less than 4, auxiliary control points can be generated to make it be 4 according to (8) as in S_0. The trajectory is as follows.

Start: the same with that of S_1.

Movement of the writing brush: $P_1 \rightarrow Q_0 \rightarrow Q_1 \rightarrow \cdots \rightarrow Q_M \rightarrow P_4(x_4, y_4, z_d - d_{min})$.

Note that Q_j $(j = 0, 1, \ldots, M)$ is the point on the B-spline curve determined by P_1 to P_4 and the width is controlled according to (6). Figure 13b shows the two variations of S_3 written by a robot hand.

3.4.5. S_4: Right falling stroke. There are two variations for S_4, one is the same with the right falling dot as in S_0, another one is given in Fig. 14a. Here, we only discuss how to write the later one. To express this stroke, five control points are

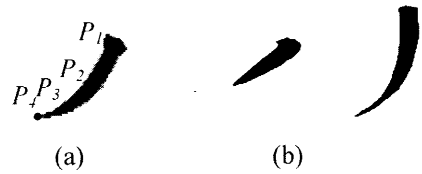

Figure 13. (a) Left falling stroke S_3. (b) Two S_3s written by a robot hand.

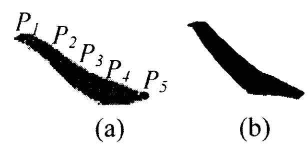

Figure 14. (a) Right falling stroke S_4. (b) S_4 written by a robot hand.

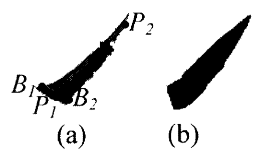

Figure 15. (a) Rising stroke S_5. (b) S_5 written by a robot hand.

necessary as given in (a). If the number of the control points between P_1 and P_4 is less than 4, auxiliary control points can be inserted to make it be 4 according to (8) as in S_0. Below is the trajectory.

Start: $B_1(x_1 - d_x, y_1 + d_y, z_d - d_{min}) \rightarrow P_1(x_1, y_1, z_d - d_{min})$ and B_1 is the same as related in S_1.

Movement of the writing brush: $P_1 \rightarrow Q_0 \rightarrow Q_1 \rightarrow \cdots \rightarrow Q_M \rightarrow P_4$.

Note that Q_j $(j = 0, 1, \ldots, M)$ is the point on the B-spline curve determined by P_1 to P_4 and the width is controlled according to (9).

End: $P_4(x_4, y_4, z_M) \rightarrow P_5(x_5, y_5, z_d - d_{min})$.

Figure 14b shows a S_4 written by a robot hand.

3.4.6. S$_5$: *Rising stroke.* Two control points P_1 and P_2 are employed to express this stroke as shown in Fig. 15a.

Start: $B_1(x_1 - 2d_x, y_1 + d_y, z_d - d_{min}) \rightarrow B_2(x_1 + 2d_x, y_1 - d_y, z_d - 1.1d) \rightarrow P_1(x_1, y_1, z_d - d)$.

Movement of the writing brush: $P_1(x_1, y_1, z_d - d) \rightarrow P_2(x_2, y_2, z_d - d_{min})$.

Figure 15b shows a S_5 written by a robot hand.

3.4.7. S$_6$: *Vertical and hook stroke.* Three control points P_1 to P_3 are employed to express this stroke as shown in Fig. 16a. R_1 is the auxiliary control point which is generated from P_2 to P_3.

Start: the same with that of S_1.

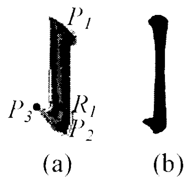

Figure 16. (a) Vertical and hook stroke S_5. (b) S_5s written by a robot hand.

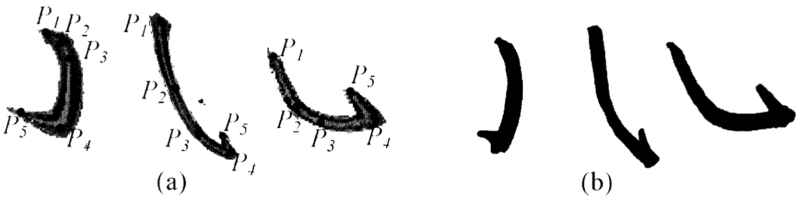

Figure 17. (a) Curved hook S_7, inclined hook S_8 and luing hook S_9. (b) S_7, S_8 and S_9 written by a robot hand.

Movement of the writing brush: $P_1(x_1, y_1, z_d - d) \rightarrow P_2(x_2, y_2, z_d - d) \rightarrow R_1(x_2, y_3, z_d - 0.9d) \rightarrow P_3(x_3, y_3, z_d - d_{min})$.

Figure 16b shows a S_6 written by a robot hand.

3.4.8. S$_7$: *Curved hook stroke;* S$_8$*: Inclined hook stroke;* S$_9$*: Lying hook stroke.* For these three strokes, at least five control points P_1 to P_5 are necessary as shown in Fig. 17a. If the number of control points between P_1 and P_4 is less than 4, auxiliary control points can be inserted to make it be 4 according to (8) as in S_0. The differences among these three strokes are how to write the starts and how to control the width of these strokes. The trajectories are given below.

Start: $B_1(x_1 - d_x, y_1 + d_y, z_d - d_{min}) \rightarrow P_1(x_1, y_1, z_d - d_{min})$, for S_7 and S_9, and B_1 is the same as related in S_1. For S_8, its start is the same with that of S_1.

Movement of the writing brush: $P_1 \rightarrow Q_0 \rightarrow Q_1 \rightarrow \cdots \rightarrow Q_M \rightarrow P_4$.

Note that Q_j $(j = 0, 1, \ldots, M)$ is the point on the B-spline curve determined by P_1 to P_4 and the width is controlled according to (6) for S_7 and S_9; for S_8, it is set at $z_d - d$.

End: $P_4(x_4, y_4, z_M) \rightarrow P_5(x_5, y_5, z_d - d_{min})$.

Figure 17 shows these three strokes written by a robot hand.

3.4.9. S$_{10}$: *Vertical and turn-right stroke;* S$_{11}$*: Vertical, turn-right and hook stroke.* These two strokes are similar. S_{11} is expressed by five control points P_1 to P_5 as shown in Fig. 18a, S_{10} by four. For S_{10}, if we think an auxiliary control point exists, and is overlapping with P_4, the control techniques for these two strokes are the same. To generate a smooth trajectory from P_2 to P_4, another auxiliary control point R_1 is put in the right side of the line P_2P_3 according to (8), where $m : n$ is set at $1 : 1$.

Start: the same with that of S_1.

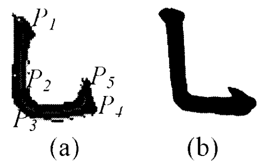

Figure 18. (a) Vertical, turn-right and hook S_{11}. (b) S_{11} written by a robot hand.

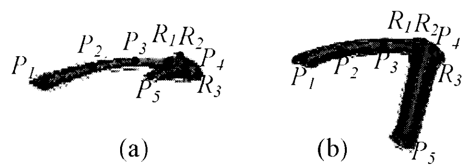

Figure 19. (a) Horizontal and hook stroke S_{13}. (b) Horizontal and fold stroke S_{14}.

Movement of the writing brush: $P_1 \to P_2 \to Q_0 \to Q_1 \to \cdots \to Q_M \to P_4$.

Note that Q_j $(j = 0, 1, \ldots, M)$ is the point on the B-spline curve determined by P_2, R_1, P_3 and P_4, and the width is set at $z_d - d$.

End: $P_4(x_4, y_4, z_M) \to P_5(x_5, y_5, z_d - d_{\min})$.

Figure 18 shows a S_{11} written by a robot hand.

3.4.10. S$_{12}$: *Vertical and rising.* This stroke can be considered as the combination of an elephant tooth in S_2 and the rising stroke S_5. Details are omitted here.

3.4.11. S$_{13}$: *Horizontal and hook stroke;* S$_{14}$: *Horizontal and fold stroke.* These two strokes can be expressed by five control points P_1 to P_5 as shown in Fig. 19. For the small S_{13} or S_{14}, it can be expressed by three control points, i.e. P_1, P_4 and P_5. In that case two auxiliary control points are inserted between P_1 and P_4 in order to generate the trajectory for it. To write the fold at P_4, three auxiliary control points R_1, R_2 and R_3 are generated from P_4. The trajectory is as follows.

Start: the same with that of S_1.

Movement of the writing brush: $P_1 \to Q_0 \to Q_1 \to \cdots \to Q_M$.

Note that Q_j $(j = 0, 1, \ldots, M)$ is the point on the B-spline curve determined by P_1, P_2, P_3 and R_1, and the width is set at $z_d - d$.

End for S_{13}: $R_1(x_4 - d_x, y_4, z_d - 0.9d) \to R_2(x_4 - d_x/2, y_4 + d_y/2, z_d - 0.8d) \to R_3(x_4 + 2d_x, y_4 - d_y, z_d - 1.1d) \to P_4(x_4, y_4, z_d - d) \to P_5(x_5, y_5, z_d - d_{\min})$.

End for S_{14}: $R_1(x_4 - d_x, y_4, z_d - 0.9d) \to R_2(x_4 - d_x/2, y_4 + d_y/2, z_d - 0.8d) \to R_3(x_4 + 2d_x, y_4 - d_y, z_d - 1.1d) \to P_4(x_4, y_4, z_d - d) \to P_5(x_5, y_5, z_d - d)$.

3.4.12. S_{15}: *Horizontal, fold and hook.* This stroke can be expressed by six control points P_1 to P_6 as shown in Fig. 20a. If the number of control points between P_2 and P_5 is less than 4, auxiliary control points are inserted according (8) as in S_0. To write the fold at P_2, three auxiliary control points R_1, R_2 and R_3 are generated from P_2. The trajectory is as follows.

Start: the same with that of S_1.

Movement of the writing brush: $P_1(x_1, y_1, z_d - d) \to R_1(x_2 - d_x, y_2, z_d - 0.9d) \to R_2(x_2 - d_x/2, y_2 + d_y/2, z_d - 0.8d) \to R_3(x_2 + 2d_x, y_2 - d_y, z_d - 1.1d) \to P_2(x_2, y_2, z_d - d) \to Q_0 \to Q_1 \to \cdots \to Q_M \to P_5$.

Note that Q_j $(j = 0, 1, \ldots, M)$ is the point on the B-spline curve determined by $P_2, \ldots, P_5$, and the width is set at $z_d - d$.

End: $P_5(x_5, y_5, z_M) \to P_6(x_6, y_6, z_d - d_{\min})$.

Figure 20 shows two S_{15}'s written by a robot hand.

3.4.13. S_{16}: *Horizontal, fold and left falling stroke.* This stroke is expressed by five control points P_1 to P_5 as shown in Fig. 21a. If the number of control points between P_2 and P_5 is less than 4, auxiliary control points are inserted according (8) as in S_0. To write the fold at P_2, three auxiliary control points R_1, R_2 and R_3 are generated from P_2. The trajectory is as follows.

Start: the same with that of S_1.

Movement of the writing brush: $P_1(x_1, y_1, z_d - d) \to R_1(x_2 - d_x, y_2, z_d - 0.9d) \to R_2(x_2 - d_x/2, y_2 + d_y/2, z_d - 0.8d) \to R_3(x_2 + 2d_x, y_2 - d_y, z_d - 1.1d) \to P_2(x_2, y_2, z_d - d) \to Q_0 \to Q_1 \to \cdots \to Q_M \to P_5$.

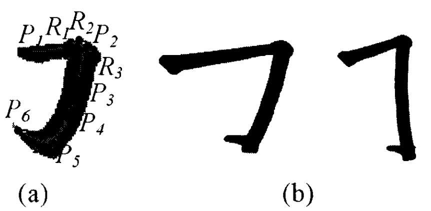

Figure 20. (a) Horizontal, fold and hook stroke S_{15}. (b) Two diffrerent S_{15}s written by a robot hand.

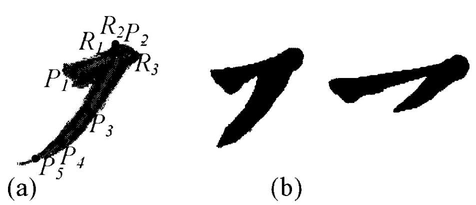

Figure 21. (a) Horizontal, fold and left falling stroke S_{16}. (b) Two diffrerent S_{16}s written by a robot hand.

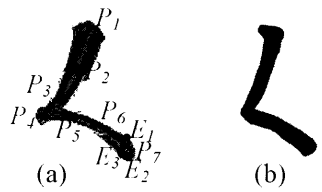

Figure 22. (a) Left falling and dot stroke S_{18}. (b) S_{18} written by a robot hand.

Note that Q_j $(j = 0, 1, \ldots, M)$ is the point on the B-spline curve determined by $P_2, \ldots, P_5$ and the width is controlled according to (6). Figure 21 shows two S_{16}'s written by a robot hand.

3.4.14. S_{17}: *Left falling and fold stroke.* This stroke can be considered as the combination of S_3 and R_5. Details are omitted here.

3.4.15. S_{18}: *Left falling and dot stroke.* This stroke is expressed by seven control points P_1 to P_7 as given in Fig. 22a. The trajectory consists of two parts, one is from P_1 to P_4 and the other from P_4 to P_7. If the number of control points for these two parts is less than 4, auxiliary control points are inserted as in S_0. To write the end, auxiliary control points E_1, E_2 and E_3 are generated from P_7. The trajectory is given below.

Start: the same with that of S_1.

Movement of the writing brush from P_1 to P_4:

$P_1(x_1, y_1, z_d - d) \to Q_0 \to Q_1 \to \cdots \to Q_M \to P_4(x_4, y_4, z_M)$.

Note that Q_j $(j = 0, 1, \ldots, M)$ is the point on the B-spline curve determined by $P_1, \ldots, P_4$ and the width is controlled according to (6).

Movement of the writing brush from P_4 to P_7:

$P_4(x_4, y_4, z_d - d) \to Q_0 \to Q_1 \to \cdots \to Q_M \to P_7(x_7, y_7, z_M)$.

Note that Q_j $(j = 0, 1, \ldots, M)$ is the point on the B-spline curve determined by $P_4, \ldots, P_7$ and the width is controlled according to (9).

End: $P_7(x_7, y_7, z_M) \to E_1(x_7 + d_x/2, y_7 + d_y/2, z_d - 0.8d) \to E_2(x_7 + d_x, y_7 - d_y, z_d - 1.1d) \to E_3(x_7, y_7 - d_y/2, z_d - d_{\min})$.

Figure 22 shows a S_{18} written by a robot hand.

3.4.16. Other strokes. Other strokes are given in Fig. 23. If we take P_t as the separation point, they are the combinations of two strokes whose trajectories are related above. The separation is given below:

$$\begin{aligned} S_{19} &= S_2 + S_1, & S_{20} &= S_1 + S_{12}, & S_{21} &= S_1 + S_8, \\ S_{22} &= S_2 + S_{15}, & S_{23} &= S_{14} + S_{16}, & S_{24} &= S_{16} + S_7, \\ S_{25} &= S_{14} + S_{15}, & S_{26} &= S_1 + S_{10}, & S_{27} &= S_2 + S_{16}. \end{aligned}$$

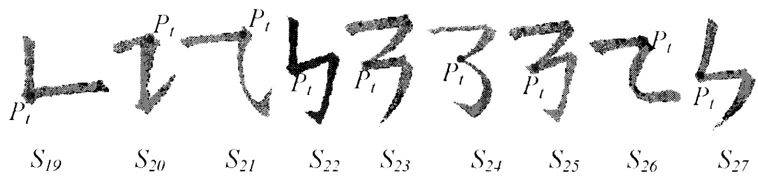

Figure 23. Strokes $S_{19}, \ldots, S_{27}$.

The trajectory at the fold point $P_t(x_t, y_t)$ is as follows, where $E_0, E_1, \ldots, E_3$ are auxiliary control points generated from P_t and E_0 is the end point of the first half of the stroke:

S_{19}, S_{22}, S_{27}: $E_0(x_t, y_t, z_d - d) \rightarrow E_1(x_t - 2d_x, y_t - d_y, z_d - d_{min}) \rightarrow E_1(x_t + 2d_x, y_t - d_y, z_d - 1.1d) \rightarrow P_t(x_t, y_t, z_d - d)$

S_{20}, S_{21}, S_{26}: $E_0(x_t - d_x, y_t, z_d - d) \rightarrow E_1(x_t - d_x/2, y_t + d_y/2, z_d - d_{min}) \rightarrow E_1(x_t + 2d_x, y_t - d_y, z_d - 1.1d) \rightarrow P_t(x_t, y_t, z_d - d)$

S_{23}, S_{25}: $E_0(x_t, y_t, z_d - d_{min}) \rightarrow E_1(x_t - 2d_x, y_t + d_y, z_d - d_{min}) \rightarrow E_1(x_t + 2d_x, y_t - d_y, z_d - 1.1d) \rightarrow P_t(x_t, y_t, z_d - d)$

S_{24}: $E_0(x_t, y_t, z_d - d_{min}) \rightarrow E_1(x_t - d_x, y_t, z_d - d_{min}) \rightarrow P_t(x_t, y_t, z_d - d_{min})$.

4. EXPERIMENTAL RESULTS

The whole system is implemented on a Windows platform and the programming language is C++. The value of T_{char} is set at 64 dots, and the threshold value for noise clump, T_n, at 6 dots. The size of the writing area T_R is set at 200 mm. The searching range, T_W, to adjust the writing order points referring to the thinned image pattern is set at 8 dots. The number of divisions, K, between two control points is set at 5. The values of d_{min} and d_{max} are determined by the writing brush. For the present writing brush, HOUSENDOU middle size, they are 12 and 30 mm, respectively. The width of the stroke, d, is set at 16 mm. Note that d is the displacement of the robot hand along the $-Z$-axis from its default position. The ratios to the width of the stroke, i.e. F_x and F_y, are set at 5. The value of the degree of inclination, δ, is summarized in Table 2. The size of the characters written by the CCC robot is given by $T_R \div T_{char} \times K_S$, where K_S is the scale coefficient which is in the range of 0.5–1.0. When K_S is set to 1.0, the robot writes the character in 200 mm × 200 mm area as shown in Fig. 6. Figure 24 shows some experimental results when K_S is set at 0.8. Figure 24a shows a photo of the final size character for 'minute', robot hand and writing brush. Other results are summarized in Fig. 24b. The first column from left in (b) shows the input image patterns of characters for 'king', 'water', 'wood', 'heart', 'woman', 'commonplace', 'no', 'moon', 'child' and 'force', from top to bottom. The second column gives the writing order denoted by the control points. The third column lists the thinned image patterns used for adjusting the positions of the control points. The fourth column shows characters written by the CCC robot.

Table 2.
Value of the coefficient of the degree of inclination

Stroke code	δ
S_0	
right inclined dot	2.2
rising dot	2.0
right falling dot	2.4
S_3	0.7
S_4	2.0
S_7	2.0
S_9	2.0
S_{16}	0.3
S_{18}	
first half	0.3
second half	−0.5

5. CONCLUSIONS

This paper relates the trajectory generation of the writing brush for a robot arm to inherit CCC techniques. First, we related the preservation of CCC and constructed a CCC database. For a character, the calligraphy writings in different styles (ancient, angular, block, semi-cursive and cursive) by different calligraphers are all registered to this CCC database. At present, this CCC database contains 29 456 characters written by famous calligraphers in Chinese history. It is able to search CCC database and restore the calligraphy writing for a specific character in this CCC database. It is also able to add new calligraphy writings to this CCC database.

Second, we mainly relate the inheritance of CCC. As CCC is not a static, but a dynamic process of an activity concerning a lot of complicated factors such as pressure control to the writing brush, speed control of the writing brush, how to write the start and end of the stroke, how to write the turn and fold on the way of the stroke, etc., we proposed to inherit this dynamic process by a robot system.

All characters can be constructed by basic strokes. There are 28 different kinds of strokes to construct all of these characters. The skeleton of a stroke is decided by the control points existing in the stroke. The shape of a stroke is determined by the trajectory derived from the control points and the pressure applied to the writing brush. The control points for 28 strokes are given and the control techniques for a robot to write these strokes in block style are developed.

The total number of Chinese characters is more than 800 000 and that in daily use is about 3500 [9]. No matter how complicated the Chinese character is, it can be constructed by the strokes in Table 1. At present, the robot can write any character in block style.

For a character, it can be written in five different styles. At present the robot can only inherit the CCC techniques for block style writing. It is necessary to make the robot be able to inherit the CCC techniques for other styles (ancient, angular, semi-cursive and cursive). These are our future work objectives. The direct application

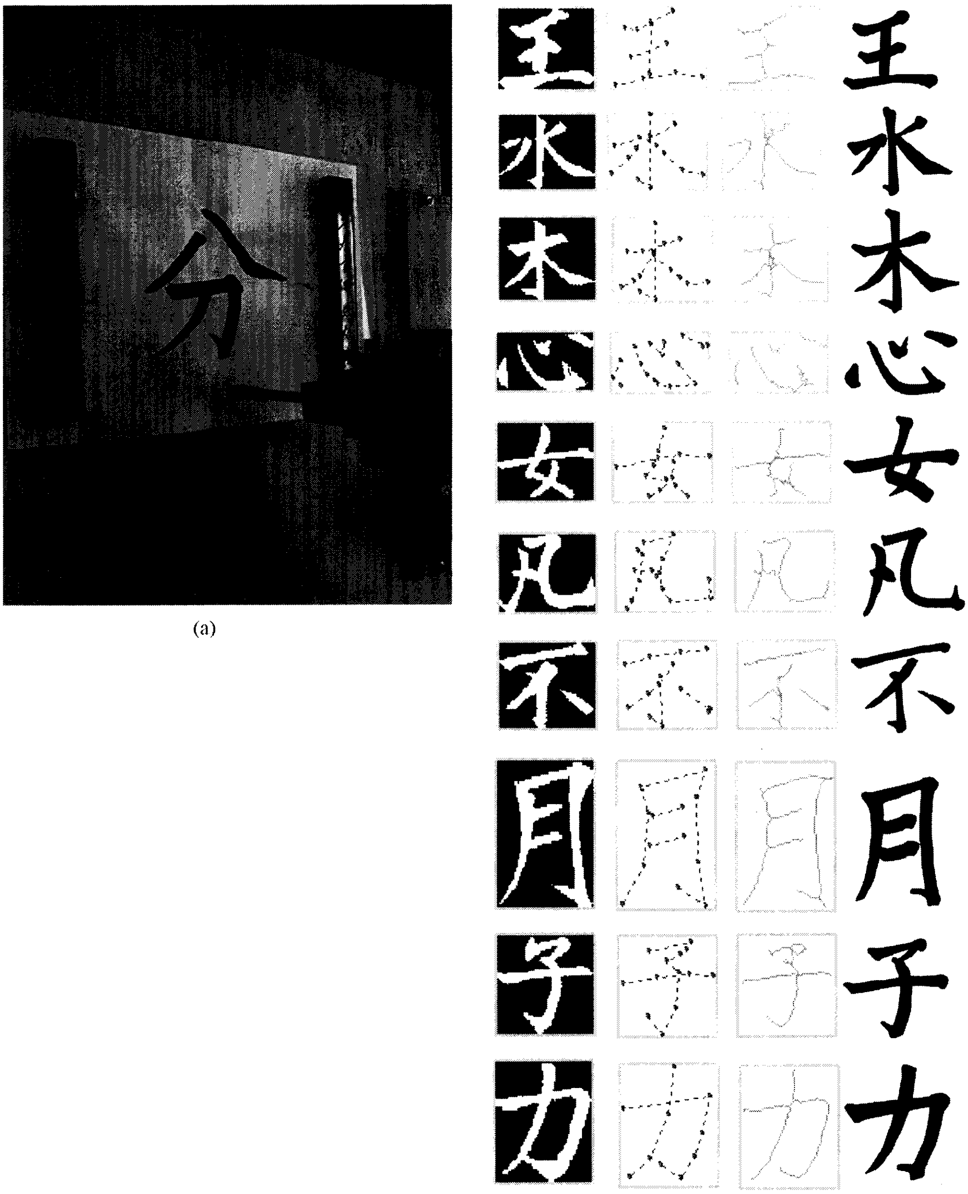

(a) (b)

Figure 24. (a) Photo of a character for 'minute' written by the CCC robot, robot hand and writing brush, at scale 0.8. (b) The first column from the left shows the input image paterns; the second, the writing order by the control points; the third, thinned image patterns used for adjusting the positions of the control points; the fourth, characters written by the CCC robot.

of this system is the design and printing of signboards. However, the main purpose of this research is to preserve and develop the CCC culture. Nowadays, with the spread of computer word processors, such as Word, Ichitaro, etc., more and more people are using them and do not like to write characters even by pen or pencil, not to mention the writing brush. Therefore, the number of competent calligraphers is becoming smaller and smaller day by day. If this situation continues for several decades, the CCC culture may face the crisis of extinction. If the robot can master all the skills of a professional calligrapher, it can do creative jobs such as making new CCC artworks. Further, the robot can instruct people in the study of calligraphy. In this way, the robot can preserve, inherit and develop the CCC culture. This is the goal we are working toward.

REFERENCES

1. F. H. Yao, G. F. Shao, R. Takaue and A. Tamaki, Development of Chinese character calligraphy robot, in: *Mechatronics and Machine Vision 2002: Current Practice*, R. S. Bradbeer and J. Billingsley (Eds), pp. 315–322. Research Studies Press, Baldock (2002).
2. N. Abo (Ed.), *Chinese Character Dictionary — From Fundamentals to Application*. Mokujisya, Tokyo (1997).
3. R. Imai (Ed.), *Fundamentals of Chinese Character Dictionary*. NHK, Tokyo (1986).
4. N. Matsuda (Eds), *Gotaijikan*. Kashiwashobo, Tokyo (1986).
5. J. Hasegawa, H. Koshimizu, A. Nakayama and S. Yokoi (Eds), *Image Processing on Personal Computer*. Gijyutsu-Hyoron, Tokyo (1986).
6. Y. Kakazu and M. Furukawa (Eds), *Fundamentals of Shape Processing Engineering*. Morikita Shupan, Tokyo (1995).
7. A. Sakurai (Ed.), *Spline Function based on C*. Tokyo Denki University Press, Tokyo (1993).
8. M. Unser, Splines — a perfect fit for signal and image processing, *IEEE Signal Process.* **16** (6), 22–38 (1999).
9. http://wenxue.tom.com/xinwen/200109/2001092503.htm

ABOUT THE AUTHORS

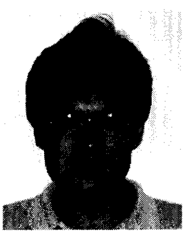

Fenghui Yao received the BE degree from Dalian Maritime University, China, in 1984, and ME and DrEng degrees from Kyushu Institute of Technology, Kitakyushu, in 1988 and 1992, respectively. From 1992 to 1994, he worked at Soliton Systems KK as a Software Engineer. He worked as a Research Associate in the Faculty of Engineering, Kyushu Institute of Technology, from 1994 to 1996. He joined University of East Asia, Shimonoseki, in 1997. He moved to Shimane University, Matsue, in 2002. Currently, he is an Associate Professor at the General Information Processing Center, Shimane University. His current research interests are image processing, intelligent mobile robots, multimedia information processing, computer architecture and parallel processing. He is a member of the IEEE, RSJ, IPSJ, IEICE and BMFSA. Currently, he is an Associate Professor at the Department of Computer Science, Tennessee State University.

Guifeng Shao received the BE degree from Wuhan University of Technology on Surveying and Mapping, China, in 1986, and ME and DrEng degrees from Kyushu Institute of Technology, Kitakyushu, in 1991 and 1995, respectively. She joined Seinan Gakuin University, Fukuoka, in 1994. She is currently an Associate Professor at Department of Commercial Science, Seinan Gakuin University. Her research interests are natural language understanding, knowledge representation, image processing, mobile robots and multimedia information processing. She is a member of the IPSJ. Currently, she is an Assistant Professor at the Department of Computer Science, Tennessee State University.

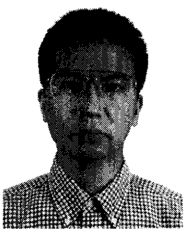

Jianqiang Yi received the BE degree from Beijing Institute of Technology, China, in 1985, and ME and DrEng degrees from Kyushu Institute of Technology, Kitakyushu, Japan, in 1989 and 1992. From 1992 to 1994, he worked at the Computer Software Development Company, Tokyo. From 1994 to 2001, he worked as a chief researcher at Mycom, Inc., Kyoto. Currently, he is a Professor in the Laboratory of Complex Systems and Intelligence Science, Institute of Automation, Chinese Academy of Sciences. His research interests include theories and applications of fuzzy control, neural networks, intelligent control, intelligent robotics, and underactuated systems.